Assessment of the Expansion of Beauharnois Dam

Luis Lacoma, Javier Rodríguez, Joaquín Martí
Principia Consulting Engineers, Madrid, Spain

Ana B. Martín
Iberdrola Generación, Madrid, Spain

Esperanza Menéndez
Eduardo Torroja Institute for Construction Sciences (IETCC), Madrid, Spain

ABSTRACT: The paper describes the contribution to the AAR benchmark of the Spanish team formed by Principia Consulting Engineers, Iberdrola Generación, and Eduardo Torroja Institute for Construction. The Beauharnois Generating Station is a large hydropower facility, with generating units spread out about a kilometre. The dam, constructed in 1932, is experiencing an expansion process caused by an AAR chemical reaction. Displacements measured at some points during the period 1973-2018 were provided by the organisers and were used to calibrate the expansion model using the general-purpose finite element program Abaqus. First, a thermal simulation was carried out to determine the periodic temperature oscillation during a representative year. The steady-state degree of saturation was also computed based on the available data. Then, mechanical models were constructed with different levels of approach. The expansion law was calibrated as a function of temperature, adopting an Arrhenius' law. The vertical displacements were used to determine an isotropic expansion rate, and the horizontal displacements to validate it. No creep was explicitly included in the models, and a crude plasticity model was defined for the concrete. The hygral conditions were assumed to eliminate the expansion when the saturation was lower than a certain threshold. The resulting displacement field appears to be reasonable for both the vertical and horizontal directions. Conservatively, the same expansion rate was assumed for the future time of interest.

1 INTRODUCTION

1.1 *Description of the dam*

The dam has an overall length of about 1400 m. Although the cross-section does not vary much along the length, the region being studied is specifically that of power unit #12 and the two adjacent units. A representative cross-section is shown in Figure 1.

Upstream from the dam the water levels may vary between 44.5 m and 46.5 m; those downstream vary between 20.461 m and 23.012 m. The calculations have been made with 46.1 m and 21.4 m, as suggested by the organisers.

The dam is made of reinforced concrete. The basic characteristics of the concrete are a compressive strength of 30 MPa, a Young's modulus of 26 GPa, and a Poisson's ratio of 0.21. The ground under the dam is rock, characterised by a Young's modulus of 30 GPa.

In the calculations described in the paper, the domain being studied, spanning the three units mentioned, is assumed to be bounded by symmetry planes on both sides.

1.2 *Problem statement*

For calibrating the models used in the analyses, the only information available consisted in histories of vertical displacements at three points and horizontal displacements at two of them; the locations of those points are marked on Figure 1. The displacements were obtained by topographic surveys conducted after 1973.

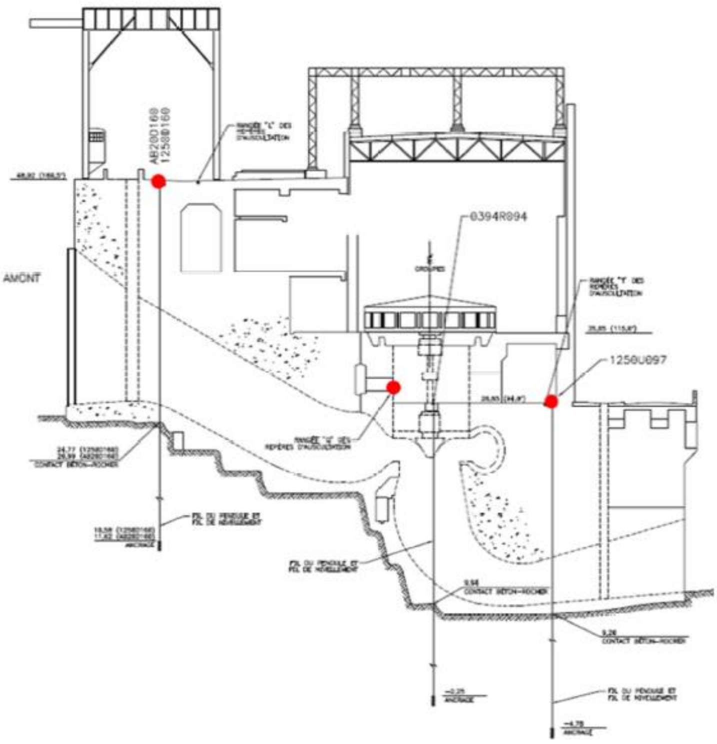

Figure 1: Representative section of a power unit

2 MODELLING APPROACH

2.1 *Geometry reconstruction*

It was found that neither the geometry nor the finite element mesh provided by the organisers were ideal for the calculations. The geometry had many undefined entities when importing it into Abaqus [5], and 20% of the mesh elements were of poor quality.

In this situation it was decided to reconstruct the geometry of the power unit with CATIA 3DEXPERIENCE [1]; the reconstructed geometry is shown in Figure 2. Also, tetrahedral meshes were generated for dealing with the different problems; examples are shown in Figure 3 for the global mesh and Figure 4 for more detailed views of the intake and power units. First-order elements were used for the thermal and hygral calculations, while second-order elements were employed in the mechanical calculations.

2.2 *Methodology*

The calculations have proceeded in several steps. The first one consisted in performing thermal analyses in order to develop a stable thermal cycle along a standard year. The hygral calculations were conducted to determine the saturation conditions at each location.

Finally, the mechanical analyses were carried out, again in several steps. In a preliminary phase, calculations were performed for only the hydrostatic and gravity loads. Already with concrete expansion, the expansion was initially assumed to be uniform and homogeneous. Then, in a second phase, the influence of temperature was incorporated and, in the final one, both temperature and moisture conditions were taken into account. The mechanical analyses included both linear and non-linear calculations.

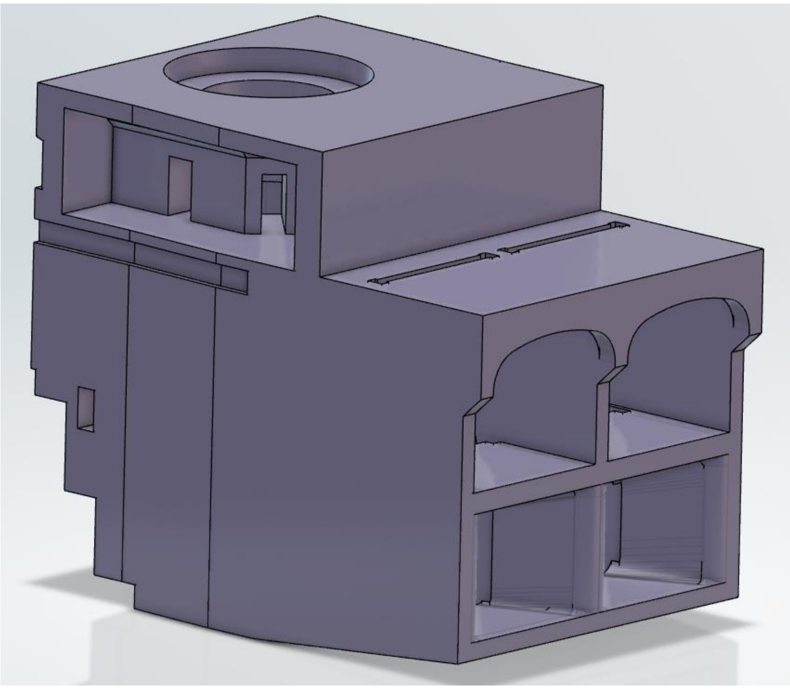

Figure 2: Reconstructed geometry

3 ENVIRONMENTAL SIMULATIONS

3.1 *Thermal analysis*

The object of the thermal analyses was to determine the evolution of the temperatures at each location during the year.

The mesh utilised in the thermal analyses included both the dam and the ground; it consisted of about 1.6 million nodes and 1.1 million first-order elements.

The analyses were performed with adiabatic boundary conditions at the ends and thermal exchanges across other surfaces with sinusoidally-varying ambient temperatures of the type (Figure 5):

$$T(d) = T_0 + A \cdot \cos(\omega d) + B \cdot \sin(\omega d), \cdot \text{where } \omega = 2\pi/365 \tag{1}$$

The analyses were conducted for a time span of 50 years to ensure a stable yearly temperature cycle at all locations. Figure 6 presents some results, namely the temperature distributions in January and July.

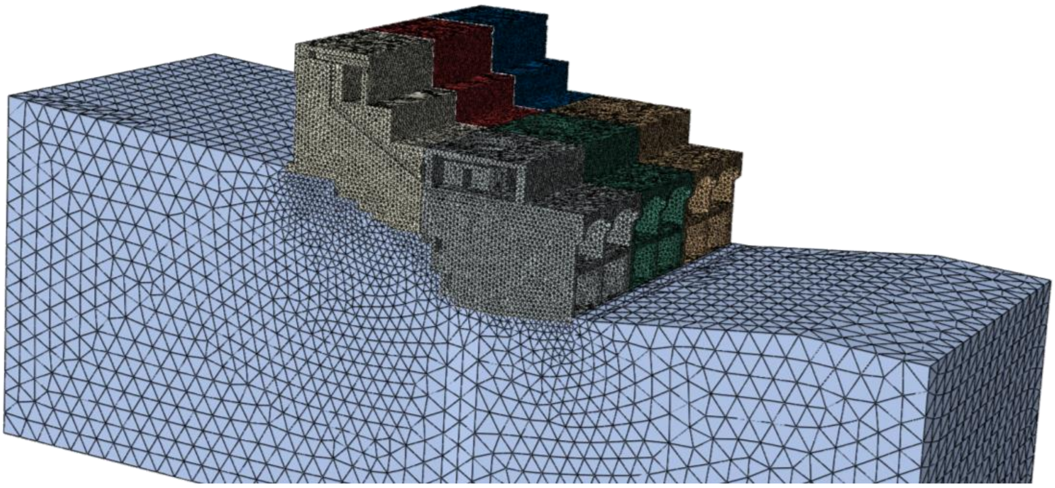

Figure 3: Representative finite element mesh

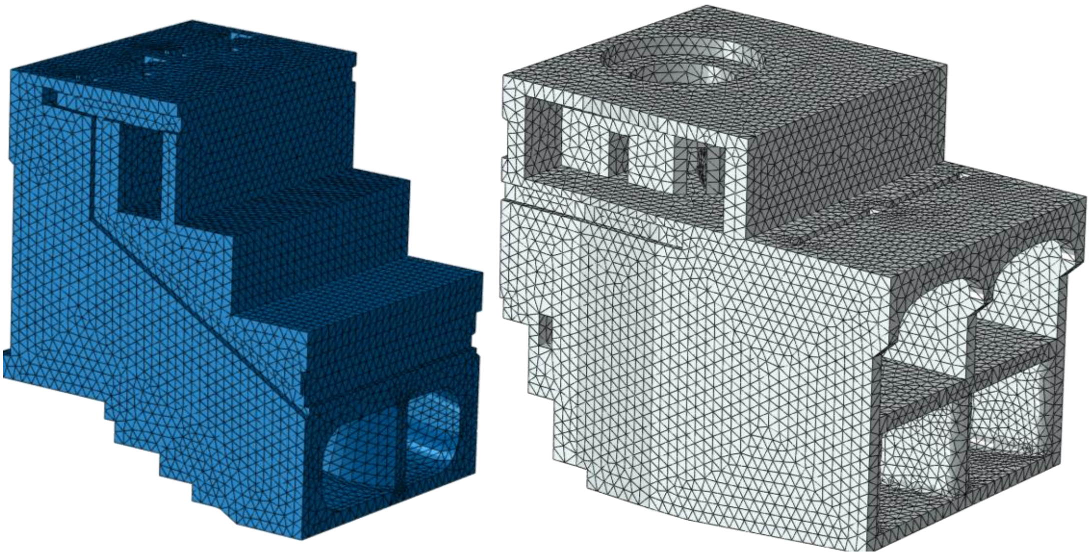

Figure 4: Detailed views of the intake and power-unit finite element meshes

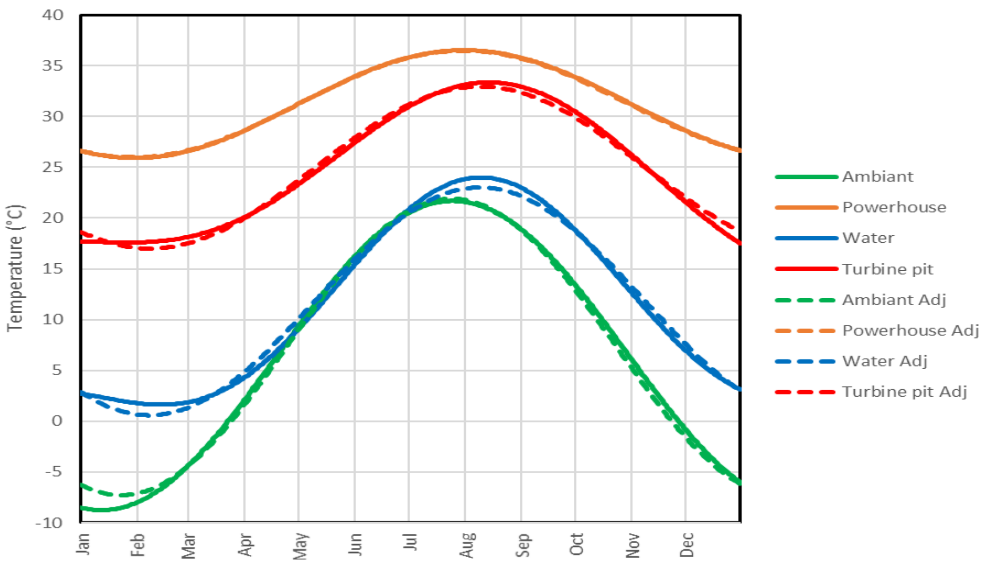

Figure 5. Harmonic fit of the season temperature for convection boundary conditions

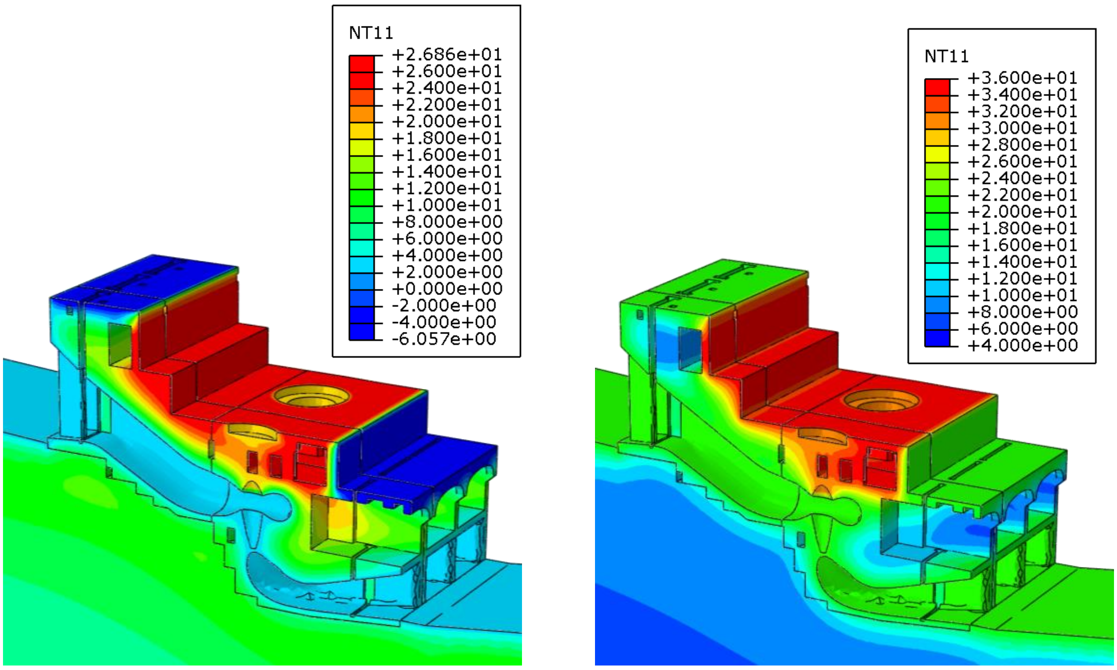

Figure 6: Temperature distribution in January (left) and July (right)

3.2 *Moisture analysis*

The mesh used for studying the moisture conditions is similar to that used in the thermal calculations, except that it only includes the body of the dam; first order elements are again used. The boundary conditions are specified in terms of pore pressures.

Capillary pressures arise when extracting particles to an unsaturated environment. The equivalent negative pressures (P_c) are approximated assuming that the ideal gas law applies, the process is isothermal, and, in equilibrium, the fraction of particles exchanged with the environment is a function of its relative humidity; more specifically, it is inversely proportional to the number of interactions between particles:

$$P_c = -\frac{\rho RT}{M} \ln h, \tag{1}$$

where ρ is the liquid density, R is the gas constant, M is the molar mass, T is the absolute temperature; and h is the relative humidity.

It is also assumed that the head loss is linear along the conduit across the dam. Concrete is characterised with its hydraulic conductivity and the capillary pressure law, both a function of the degree of saturation (Figure 7).

According to Mualem's model, as described in [2], the relative hydraulic conductivity (or permeability for Darcy's law) depends on the degree of saturation (Θ) and the tortuosity, the latter being a function of the pressure and the water content ($h(x)$):

$$K_r = \Theta^{1/2} \left[\int_0^{\Theta} \frac{1}{h(x)} \mathrm{d}x \Big/ \int_0^1 \frac{1}{h(x)} \mathrm{d}x \right]^2 \tag{2}$$

The phenomenological retention law is assumed to hold (with a logistic "S" shape)

$$\Theta = \left(\frac{1}{1+(\alpha h)^n} \right)^m \tag{3}$$

Conveniently $m = 1 - 1/n$ and the conductivity can be integrated explicitly, yielding

$$K_r = \Theta^{1/2} \left[1 - \left(1 - \Theta^{1/m} \right)^m \right]^2. \tag{4}$$

When the problem is analysed, using the previous hypotheses, the resulting distribution of the degree of saturation is that shown in Figure 8.

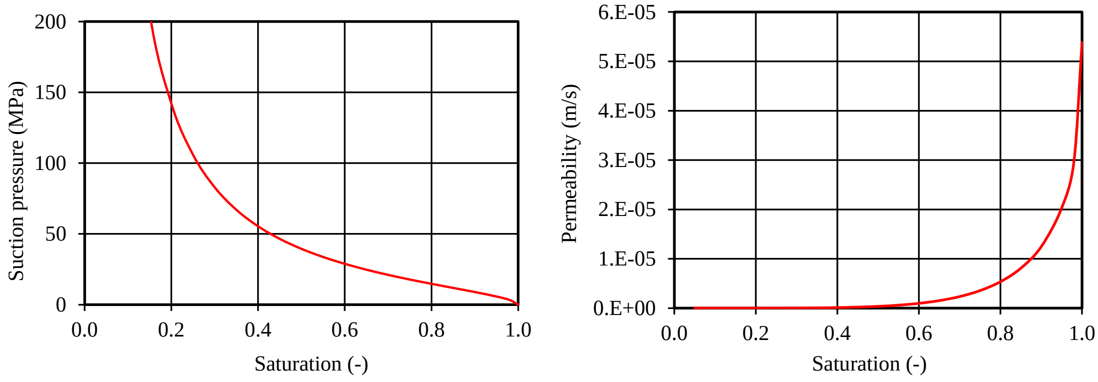

Figure 7: Suction pressure and permeability as a function of the degree of saturation

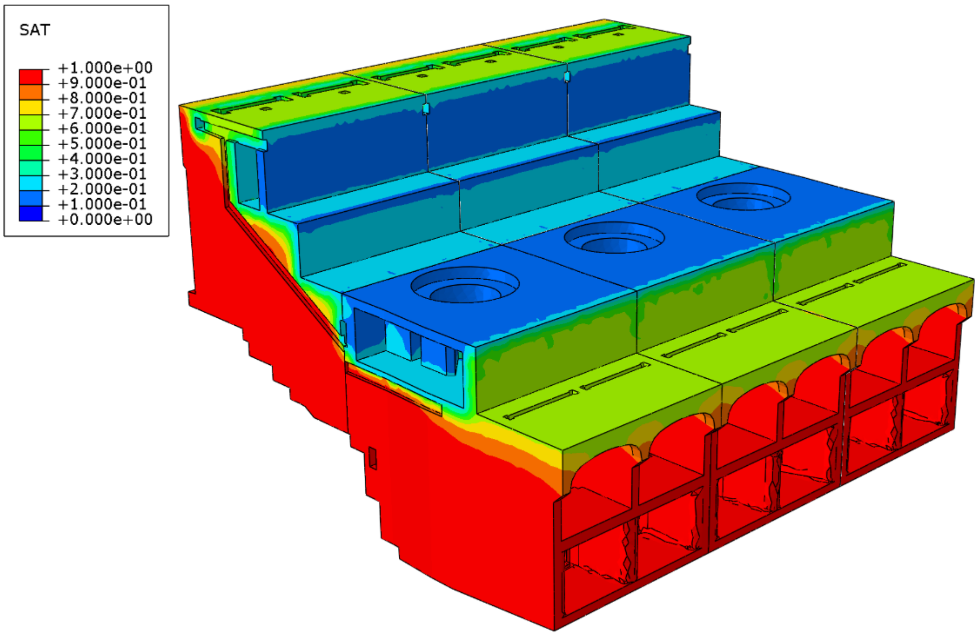

Figure 8: Distribution of the degree of saturation

4 MECHANICAL ANALYSIS

4.1 *Estimation of the expansion rate*

A first mechanical analysis was conducted to determine the displacements that would result from a given uniform expansion at the locations where its evolution was known. This was done using a mesh with about 740,000 second-order elements, 1.1 million nodes and 3.4 million dof's, provided with displacement boundary conditions.

The problem is linear, and a 0.1% uniform expansion was used. The annual displacement rate calculated for the homogeneous expansion is shown in Figure 9. The results allowed calibrating the expansion using the vertical displacement rates derived from the measurements: 0.984 mm/yr at the “Crest”, 0.567 mm/yr at the “Turbine floor” and 0.479 mm/yr at the “Turbine pit”. The estimated linear (not volumetric) expansion rate is $2.8 \cdot 10^{-3}$ %/year.

4.2 *Evolution of the expansion*

The chemical reaction is affected by temperature. Consistently, a steady-state, isotropic expansion model was established including the temperature dependence. The mechanical model did not incorporate creep, as it is difficult to separate from the expansion on the basis of the information available; also, as suggested by the benchmark organisers, thermal expansion was not considered in the calculations.

It was assumed that the annual rate of chemical expansion is a function of the yearly temperature cycle. The instantaneous rate was taken to be proportional to *exp(T/U)* with a factor *f*:

$$\dot{\varepsilon}_{\mathrm{AAR}} = f \exp(T/U), \tag{5}$$

where U is an activation energy; the value given was 5400 K, taken from Larive [3] for the characteristic reaction time. The expansion tends to homogeneous as this value grows. An additional analysis was performed with 9400 K, given by Larive for the latency time, but the results were less satisfactory.

The simulation was carried out using the temperatures, updated every 15 days, in an Abaqus subroutine. The factor multiplying the exponential function was calibrated to achieve an annual expansion rate that coincides with the average rate recorded (written at the end of the previous section 4.1), and the result was $f = 11.4$ day^{-1}.

With the calibrated expansion model, the evolution was simulated for a period of 115 years (the total period of analysis required by the organisers is 2067 - 1932 = 135 year but no expansion is assumed during the first 20 years). The analysis times could be reduced by using in subsequent years information produced in the first year of expansion. The initial evolution of the dam is not well known, as the displacement records start in 1973, some 40 years after construction. A latency time of 20 years was assumed, based on the authors' experience on other dams.

A crude von Mises model was used to approximate some of the effects of plasticity. This should improve the accuracy of the reactions calculated between the various blocks and the foundation. The calculated distribution of the expansion rate appears in Figure 10. The reactions were calculated with an Abaqus tool that integrates the nodal forces.

4.3 *Effect of the degree of saturation*

To incorporate the effects of moisture, the strategy adopted consisted in eliminating the expansion when the degree of saturation is below 0.3. Figure 11, coming from a different project, shows representative stereomicroscopic images of the gel in concrete pores. In the images the porous are filled with a vitreous gel and surrounded by an aqueous gel; a value of 0.3 may be representative of the ratio of both volumes, and it is deemed reasonable as a threshold of the saturation degree to supress the macroscopic expansion. The factor multiplying the temperature-dependent exponential function (*f*) was still considered appropriate and was not recalibrated. The expansion distribution is also shown in Figure 10.

The comparison of the displacement histories, considering the effects of temperature and saturation, is provided in the next two figures: Figure 12 for the vertical displacements and Figure 13 for the horizontal ones. Notice that only the vertical displacements had been used for calibration purposes; also, since the origins are not known, the experimental curves were arbitrarily shifted for comparison purposes.

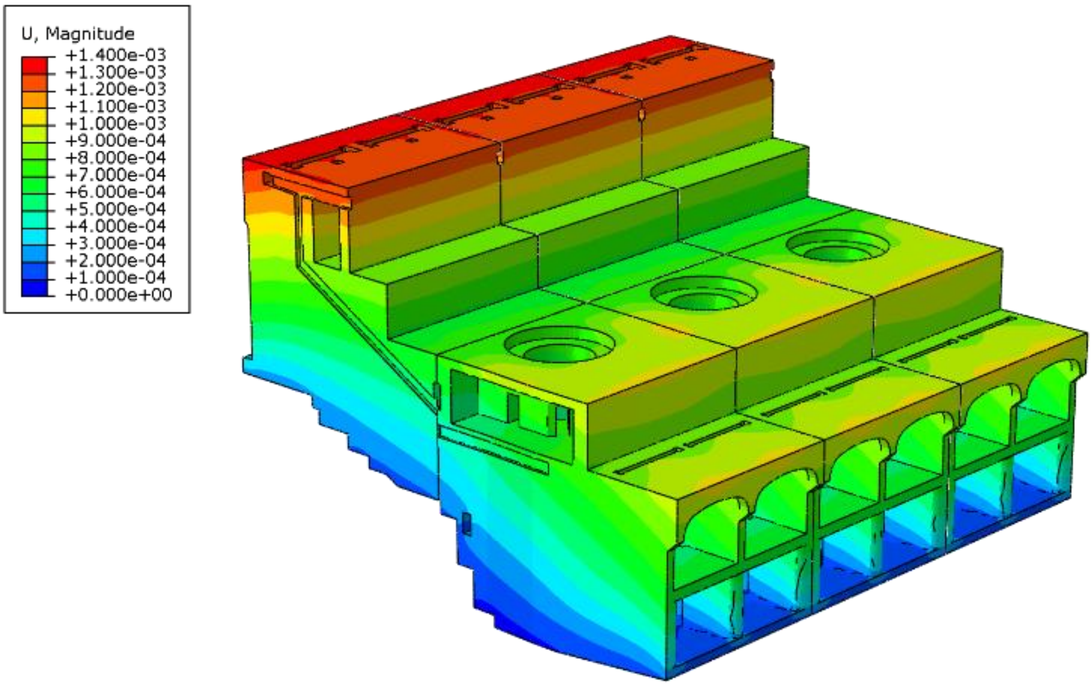

Figure 9: Annual displacement increment (m) for homogeneous expansion of $2.8 \cdot 10^{-3}$ %/year

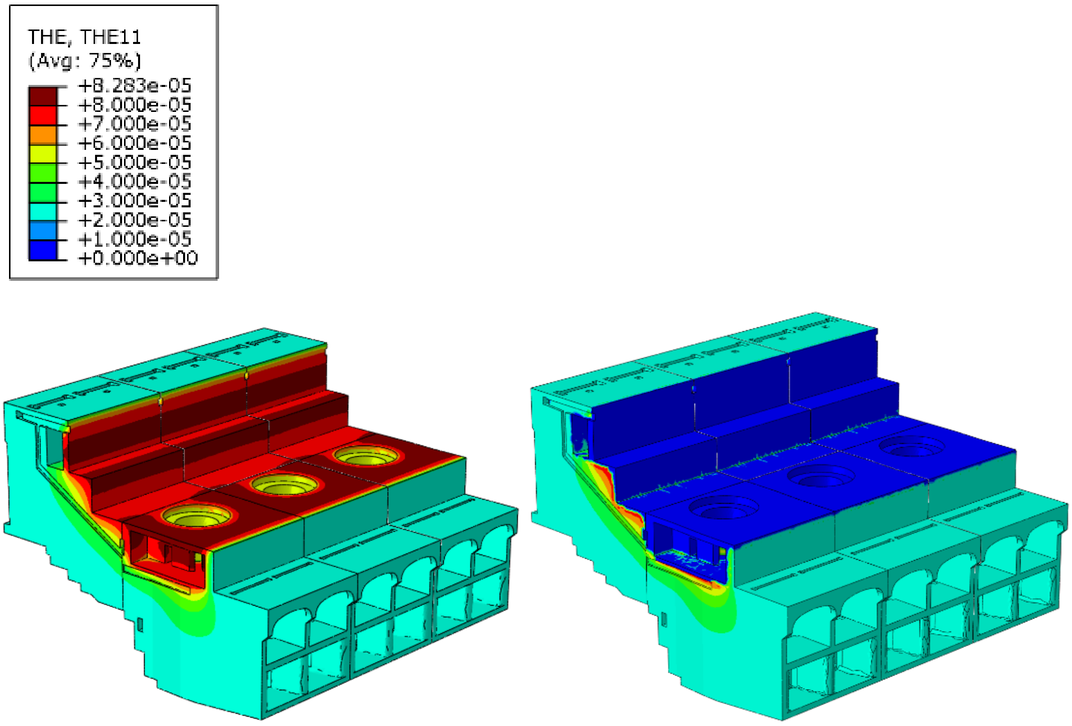

Figure 10: Distribution of the expansion rate without (left) and with dependence on the saturation degree

Figure 11: Representative stereomicroscopic images

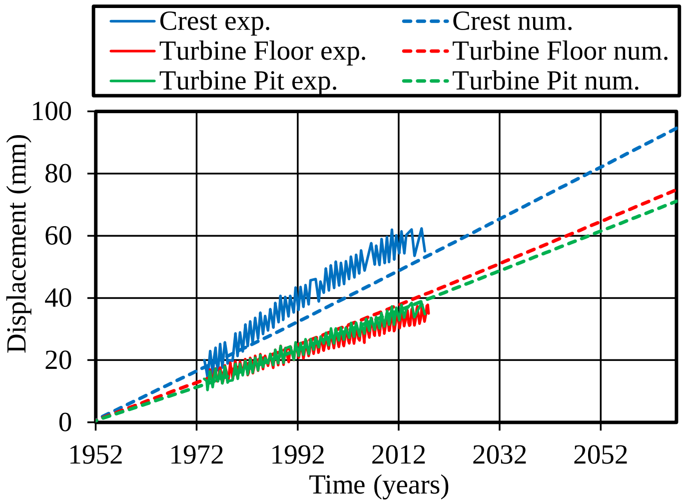

Figure 12: Histories of vertical displacements of the control points (moisture dependent)

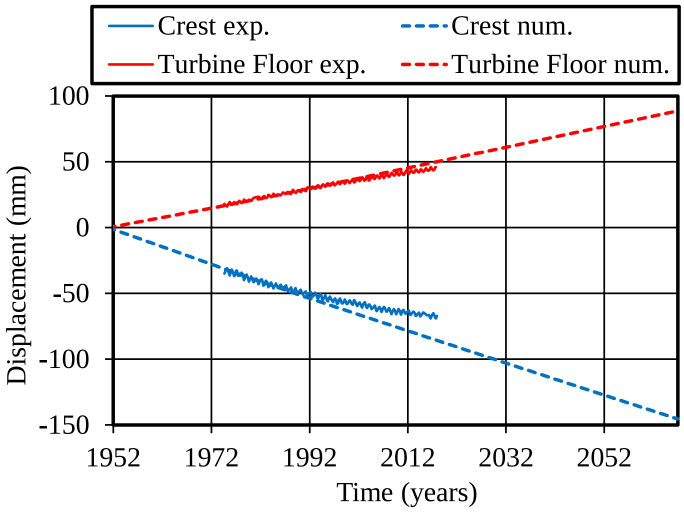

Figure 13: Histories of horizontal displacements of the control points (moisture dependent)

5 DISCUSSION AND CONCLUSIONS

State-of-the-art simulation tools have been used to analyse the state of a dam affected by chemical expansion. Additional experimental information, regarding both the material characterisation (e.g., according to [6]) and the structure, would be required for more conclusive results and to validate possible strategies and remedial measures; in any case, the exercise proposed by the organisers is deemed very useful for illustrating the different analysis methodologies.

With the available information, it is difficult to predict the future evolution of the expansion rate, which has been assumed to remain constant after a latency time following construction; this is typically a conservative assumption. The temperature dependence is introduced via an Arrhenius' law, using published activation energies of AAR.

Based only on displacement information, the creep and chemical effects cannot be decoupled. Conveniently, a viscoelastic model is not defined, and an effective expansion is calibrated.

There is no consensus about how to consider the effect of the degree of saturation; moreover, there are large uncertainties its value in concrete affected by AAR. Our approach consisted in simply supressing the expansion when the value is below 0.3; this threshold is considered reasonable, based on both micromechanics and sensitivity considerations.

The calibration was only based on the vertical displacements, but the computed horizontal displacement rates also turned out to be consistent with the data. A stress-dependent anisotropic expansion model could be assessed for improving the simulation.

It is possible to model the rebars, typically with truss elements embedded in the solid domain, characterised with a concrete inelastic model. But, in the context of the present exercise, this would not be expected to improve significantly the predictive capabilities of the model.

The rest of the information requested by the benchmark organisers has also been provided.

6 REFERENCES

[1] Dassault Systèmes. '*3DEXPERIENCE User Assistance. 3D Modeling. Mechanical Design*'. 2021.

[2] M. Th. van Genuchten 1980 'A Closed-form Equation for Predicting the Hydraulic Conductivity of Saturated Soils', In: *Soil Science Society of America Journal*. 44.5 (1980), pp. 892-898, doi: 10.2136/sssaj1980.03615995004400050002x

[3] C. Larive. '*Apports combinés de l'experimentation et de la modelélisation à la compréhension de l'alcali réaction et ses effets mécaniques*'. Études et Recherches des LPC OA 28. Laboratoire Central des Ponts et Chaussées, Paris, France, 1998.

[4] S. N. Roth and B. Miquel. 'Theme B: AAR Affected Dam. Evaluation and Prediction of the Behaviour of the Beauharnois Dam'. In: *16th International Benchmark Workshop on Numerical Analysis of Dams, Ljubljana, Slovenia*, 2022.

[5] SIMULIA. '*Abaqus Analysis User's Guide'*. 2021.

[6] A. B. Martín, E. Menéndez and L. M. Lacoma. 'Nueva Metodología para la Predicción de la Expansión del Hormigón en Presas con RAA'. In: *XI Spanish Conference on Large Dams, León, Spain*, (2018), pp. 1-10.